Calibration of Airdata Systems Using Extended Kalman Filtering Technique

Majeed M[a,1], Indra Narayan Kar[b]
[a]Scientist, National Aerospace Laboratories, Kodihalli, Bangalore
[b]Professor, Department of Electrical Engineering, IIT Delhi

Abstract

One of the aims of air data systems is the determination of flight parameters angles of attack and angle of sideslip from measurements of local pressures and of local flow angles on wings or fuselage using a proper set of sensors. The active and integrated use of flight parameters in a full-authority flight control system imposes requirements for accurate and reliable air data, which are critical to maintain control. In this paper, a methodology based on the data fusion using Extended Kalman Filter technique is applied to dynamic maneuvers with rapid variations in the aircraft motion to calibrate angle of attack and angle of sideslip. The main goal of the investigations reported in this paper is to obtain online accurate flow angles from the measured vane deflection and difference pressures from probes sensitive to flow angles even in the adverse effect of wind or turbulence. The investigations are initially made on simulated flight data with wind and turbulence effects and it is showed that both alpha and beta estimates are accurate. The same procedure is then extended to flight test data of a high performance fighter aircraft. It has been shown using these results that sensor data fusion approach proposed in this paper is of great value in online implementation.

Key words: Airdata Systems, Sensor Data Fusion, Extended Kalman filtering

1. INTRODUCTION

Air data systems are required on aircraft as part of the flight control system. Typically these systems require some form of airdata sensors. These airdata sensors installed on high performance modern aircraft must be carefully calibrated to achieve accurate onboard airdata measurements of angle of attack (AoA /α) and angle of sideslip (AoSS/β) [1,2,3]. Accuracy of these measurements should be always pursued for a multitude of tasks, including in-flight simulation, flight safety and aircraft performance evaluation, but also air traffic control and navigation. These airdata measurements are affected by several flight variables that may vary over a very wide range; thus, air-data sensors calibration must be treated as a multidimensional and nonlinear problem [4,5].

A recent research study uses a detailed aerodynamic model of the aircraft within an Extended Kalman Filter-(EKF) framework [6] and offers potential to eliminate the sensors required to measure AoA & AoSS. Today's modern computers have the computational throughput to functionally estimate these parameters accurately, thus eliminating these sensors, or at a minimum providing a functional backup for improved reliability. Unfortunately, there is no way to use such estimation framework prior to the validation of aerodynamic database consisting of force and moment coefficients, because estimation accuracy is directly tied to the aerodynamic data base accuracy [6]. This is because the models of aerodynamic forces, propulsive forces, and moments are embedded in the EKF formulation. So, measurements of AoA and AoSS are primary requirements for the aircraft, which does not have the valid aerodynamic database. For an angle with multiple sensors, sensor fusion algorithms yield good results since the fusion of data from multiple sensors results in both qualitative and quantitative benefits [7,8,9].

Email addresses: majeed_md_123@rediffmail.com (First Author),
ink@ee.iitd.ac.in (Second Author),
URL: http://www.aero.iisc.ernet.in (First Author)
[1]Corresponding author

Moreover, the effectiveness of another approach say Kalman Filter algorithm incorporating GPS [2,10] for real time airdata calibration is directly dependent on the GPS error associated as uses differential GPS (DGPS) position and velocity data to form the measurements. GPS has the advantages of all weather, globality and consistently high precision. But data update rate of a GPS receiver is low (normally at 1Hz) and the performance is dependent on the number and geometry of satellites being tracked. In comparison, the proposed approach in our paper overcomes this deficiency because multiple air data sensors outputs are taken as measurements. By fusing valuable information from sensors into the EKF algorithm helps in estimating each sensor's calibration parameters separately in terms of sensor offset error and sensitivity factor.

Fusion processes are often categorized as low, intermediate or high level fusion depending on the processing stage at which fusion takes place. Low-level fusion, also called data fusion, combines several sources of raw data to produce new raw data that is expected to be more informative and synthetic than the inputs. There are two approaches for fusion of multiple sensor data: measurement fusion and state vector fusion. In measurement fusion, sensor measurements are combined and an optimal estimate of target state vector is obtained. Since this approach is optimal and theoretically superior to state vector fusion [11], measurement fusion approach is employed here. Currently there exist two commonly used measurement fusion methods for Kalman-filter-based multi sensor data fusion. The first (Method I) simply merges the multi sensor data through the observation vector of the Kalman filter, whereas the second (Method II) combines the multi sensor data based on a minimum mean square error criterion. It is worth noting that proposed flow angle sensors are dissimilar since AoA senses by different sensors vane and pressure probe, while AoSS senses by nose boom pressure probe and side air data pressure probe. In such case, measurement fusion method II is not applicable to use [12]. Therefore, measurement fusion method I applied to estimate the flow angles from the flight data.

The primary aim of the presented data fusion approach for air data calibration is to accurately estimate airdata parameters or to make inferences that may not be feasible from a single sensor alone as in flight path reconstruction (FPR) using EKF [8,13,14]. In addition, reduced ambiguity, increased confidence and improved system reliability are the main benefits applicable to majority of the data fusion applications. In our approach, we have also given the special attention for presence of turbulence

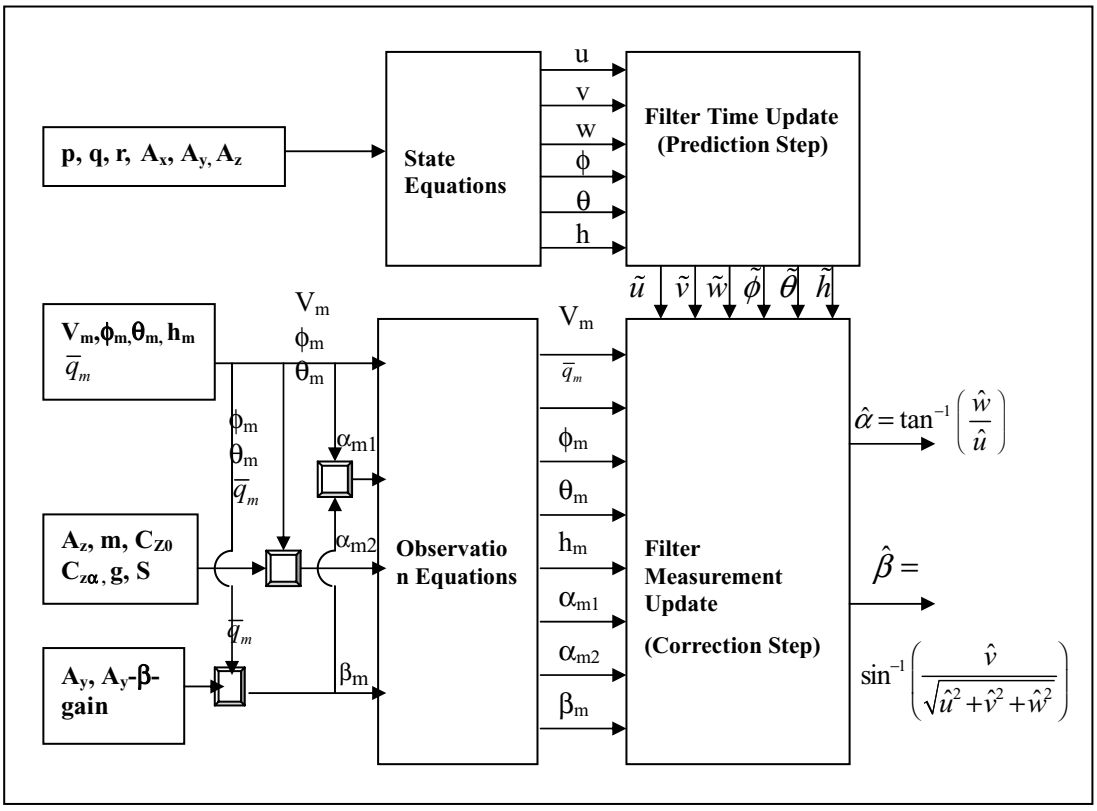

Figure 1. AoA-AoSS Estimation Scheme using Extended Kalman Filter

during the flight maneuvers. These methods are applied to flight data of a high performance fighter aircraft. Major contribution occurs in situations where there is a significant sensors noise property variation. A FPR using output error method (OEM) are also applied to analyze the flight maneuvers and to calibrate AoA and AoSS [15]. It helps to reconfirm the result obtained from EKF based sensor fusion real time approach, by comparing these results with standard offline method like FPR using OEM [16].

In the following section, the sensor fusion approach is applied to dynamic maneuvers with rapid variations in the aircraft motion to calibrate the flow angles (α & β). This approach is model based data level measurement fusion using EKF and has been properly formulated from a FPR problem. The main goal of the investigations is to obtain online accurate flow angles from the sensor measurements even with the adverse effects of wind or turbulence.

2. DESIGN EQUATIONS FOR AOA-AOSS ESTIMATION USING EKF

The AoA-AoSS Estimation algorithms are based on the nonlinear 6DOF equations of motion, kinematics and navigation equation within an EKF that processes measurements of airdata parameters from multiple sensors. Figure1illustrates AoA-AoSS Estimation Scheme using Extended Kalman filter. The AoA-AoSS Estimation algorithms include EKF algorithm, 6DOF model (state equations) and measurement model (observation equations).

2.1. Extended Kalman Filter Algorithm

One of the most popular forms of representing aircraft equations of motion in the time domain is the state space form [17]. The dynamic and measurement model is assumed to be described by the following continuous-discrete state space models:

$$\begin{aligned} &\dot{\mathbf{x}}(t) = \mathbf{f}\left[\mathrm{x}(t), \mathbf{u}(t), \mathrm{w}(t)\right] \quad \mathbf{y}(t) = \mathbf{h}\left[\mathrm{x}(t)\right] \\ &\mathbf{z}(k) = \mathbf{y}(k) + \mathbf{v}(k) \qquad \mathbf{x}(0) = \mathbf{x}_0 \end{aligned} \tag{1}$$

Functions $\mathbf{f} \in \Re^{\mathrm{n}}$ and $\mathbf{h} \in \Re^{\mathrm{m}}$ are general nonlinear functions; vector $\mathrm{x} \in \Re^{n}$ is the state vector; $\mathbf{u} \in \Re^{1}$ is the input/control vector; $\mathbf{y} \in \Re^{\mathrm{m}}$ is the output vector, and $\mathbf{z} \in \Re^{\mathrm{m}}$ is sampled at discrete points with a uniform Δt sampling time; vectors **w** and v are process and measurement noises and have covariance matrices **Q** and **R**, respectively. More precisely, noises are considered to be zero mean, white, and with Gaussian distribution. They are also assumed to be independent between themselves and also with respect to the initial condition **x**(0), that is,

$$\begin{aligned} &E\{\mathbf{w}(k)\} = 0 \quad E\{\boldsymbol{v}(k)\} = 0; \quad E\left\{\mathbf{w}(k)\mathrm{w}(j)^{T}\right\} = \mathbf{Q}\delta(k-j) \\ &E\left\{\boldsymbol{v}(k)\boldsymbol{v}(j)^{T}\right\} = \mathbf{R}\delta(k-j); \quad E\left\{\mathbf{w}(k)\boldsymbol{v}(j)^{T}\right\} = 0 \\ &E\left\{\mathbf{x}(0)\mathbf{w}(k)^{T}\right\} = 0 \quad E\left\{\mathbf{x}(0)\boldsymbol{v}(k)^{T}\right\} = 0 \end{aligned} \tag{2}$$

The standard Kalman filter addresses only linear stochastic systems and it is not directly applicable to nonlinear problems. On the other hand, there are no practical solutions for the general optimal nonlinear problem. An artifice to use the Kalman filter equations in a nonlinear problem, with nonlinearities either in the dynamic or in the measurement model, is to linearize the system around the current state estimate. This approach is named the extended Kalman filter. For this purpose, a corresponding linear system is derived from the original one by calculating all necessary Jacobians. When model parameters are to be estimated simultaneously, a new state vector is then defined based on the previous state vector and on the proposed parameter vector, therefore resulting in the EKF augmented state vector.

The linearized system is calculated based on (1) through the following derivatives with the jacobians defined in (3).

$$\begin{aligned} &\mathbf{A}(k) = \frac{\partial \mathbf{f}(\mathbf{x}(t), \mathbf{u}(t), 0)}{\partial \mathbf{x}}\bigg|\hat{\mathbf{x}}(k); \quad \mathbf{B}(k) = \frac{\partial\, \mathbf{f}(\mathbf{x}(t), u(t), 0)}{\partial \mathbf{u}}\bigg|\hat{\mathbf{x}}(k) \\ &\mathbf{C}(k) = \frac{\partial\, \mathbf{h}(\mathbf{x}(t))}{\partial \mathbf{x}}\bigg|\mathbf{x}(k) \end{aligned} \tag{3}$$

The state transition matrix $\mathbf{\Phi}$ and its integral $\mathbf{\Psi}$ at each discrete point are given by

$$\begin{aligned}\mathbf{\Phi}\ (k+1) &= I + \mathbf{A}(k)\Delta t + \mathbf{A^2}(k)\frac{\Delta t^2}{2!} + \cdots \\ \mathbf{\Psi}\ (k+1) &= I\Delta t + \mathbf{A}(k)\frac{\Delta t^2}{2!} + \mathbf{A^2}(k)\frac{\Delta t^3}{3!} + \cdots\end{aligned} \tag{3}$$

By calculating the transition matrix Φ and its integral Ψ, the standard Kalman filter equations can then be used. As it is well known, the algorithm can be divided into two steps [18]: time propagation and measurement correction. These steps are usually named as "prediction" and "correction" respectively. Initial state $\hat{x}(0)$ and covariance matrix $\mathbf{P}(0)$are assumed at first and then are propagated using [19]

$$\begin{aligned}\tilde{\mathbf{x}}(k+1) &= \hat{\mathbf{x}}(k) + \int_{t_k}^{t_{k+1}} \mathbf{f}(\mathbf{x}(t), \bar{\mathbf{u}}_m(t), 0)\, dt \\ \tilde{\mathbf{P}}(k+1) &\approx \Phi(k+1,k)\hat{P}(k)\,\Phi^T(k+1,k) + \\ &\quad \Psi(k+1,k)\mathbf{B}(k)\mathbf{Q}(k)\mathbf{B}^T(k)\,\Psi^T(k+1,k)\end{aligned} \tag{4}$$

where $\bar{\mathbf{u}}_m$ is the average input between the two consecutive samples. The covariance prediction step in (4) is valid for input noise. It is worth mentioning here that the $\mathbf{Q}$ matrix in the compatibility check context represents the input noise rather than the process noise.

The propagation is done until more information is available from the sensors. This is the correction phase and it updates, based on the Kalman gain and on the innovations, states and covariance as

$$\begin{aligned}\mathbf{K}(k) &= \tilde{\mathbf{P}}(k)\,\mathbf{C}^T(k)\left[\mathbf{C}(k)\,\tilde{\mathbf{P}}(k)\,\mathbf{C}^T(k) + \mathbf{R}(k)\right]^{-1} \\ \hat{\mathbf{x}}(k) &= \tilde{\mathbf{x}}(k) + \mathbf{K}(k)\left[\mathbf{z}(k) - \mathbf{h}\{\tilde{\mathbf{x}}(k)\}\right] \\ \hat{\mathbf{P}}(k) &= \left[\mathbf{I} - \mathbf{K}(k)\,\mathbf{C}(k)\right]\tilde{\mathbf{P}}(k)\end{aligned} \tag{5}$$

2.2. System Dynamic and Measurement Models

To summarize the system dynamic and measurement models, it must be noted that all calibration parameters are considered as random walk and incorporated into the state vector, via state augmentation. These groups of first order differential equations are necessary to characterize the aircraft motion and are available in most of the text books [19]. The full dynamic model is represented by

$$\begin{aligned}
&\dot{u} = -(q_m - \Delta q)w + (r_m - \Delta r)v - g\sin\theta + A_x^{CG}, && u(t_0) = u_0 \\
&\dot{v} = -(r_m - \Delta r)u + (p_m - \Delta p)w + g\cos\theta\sin\phi + A_y^{CG}, && v(t_0) = v_0 \\
&\dot{w} = -(p_m - \Delta p)v + (q_m - \Delta q)u + g\cos\phi\cos\theta + A_z^{CG}, && w(t_0) = w_0 \\
&\dot{\phi} = (p_m - \Delta p) + (q_m - \Delta q)\sin\phi\tan\theta + (r_m - \Delta r)\cos\phi\tan\theta, && \phi(t_0) = \phi_0 \\
&\dot{\theta} = (q_m - \Delta q)\cos\phi - (r_m - \Delta r)\sin\phi, && \theta(t_0) = \theta_0 \\
&\dot{h} = u\sin\theta - v\sin\phi\cos\theta - w\cos\phi\cos\theta, && h(t_0) = h_0
\end{aligned} \tag{6}$$

where p, q, and r are the projection of the angular rate vector along the aircraft body axis and their biases in measurements are defined by $(\Delta p, \Delta q, \Delta r)$; θ and ϕ are, respectively, the pitch and the roll angles; u, v, w are inertial speed projections along the aircraft body axis. The linear accelerations

($A_x^{CG}, A_y^{CG}, A_z^{CG}$) at the CG are computed from the accelerations ($A_{xm}^{AS}, A_{ym}^{AS}, A_{zm}^{AS}$) measured by the acceleration sensor at a point away from the CG through the following relation [19]:

$$\begin{aligned} A_x^{CG} &= a_{xm}^{AS} + (q^2 + r^2)x_{ASCG} - (pq - \dot{r})y_{ASCG} - (pr + \dot{q})z_{ASCG} - \Delta A_x \\ A_y^{CG} &= a_{ym}^{AS} + (pq + \dot{r})x_{ASCG} + (p^2 + r^2)y_{ASCG} - (qr - \dot{p})z_{ASCG} - \Delta A_y \\ A_z^{CG} &= a_{zm}^{AS} - (pr - \dot{q})x_{ASCG} - (qr + \dot{p})y_{ASCG} + (p^2 + q^2)z_{ASCG} - \Delta A_z \end{aligned} \tag{7}$$

Here ($x_{ASCG}, y_{ASCG}, z_{ASCG}$) denote the position of the accelerometer with respect to the CG in the body-fixed coordinates; the biases in the measurement of ($A_{xm}^{AS}, A_{ym}^{AS}, A_{zm}^{AS}$) are denoted by ($\Delta A_x, \Delta A_y, \Delta A_z$).

The measurement equations are given by:

$$\begin{aligned} V_m &= \sqrt{u^2 + v^2 + w^2} + \eta_v; \\ \bar{q}_m &= \frac{1}{2}\rho\left(u^2 + v^2 + w^2\right) + \Delta\bar{q} + \eta_{\bar{q}}; \\ \phi_m &= \phi + \eta_\phi; \\ \theta_m &= \theta + \eta_\theta; \\ h_m &= h + \eta_h; \\ \alpha_{vane} &= K_{\alpha 1} \cdot \tan^{-1}\left(\frac{w_{vane}}{u_{vane}}\right) + \Delta\alpha_1 + \eta_{\alpha_{vane}}; \\ \alpha_{spb} &= K_{\alpha 2} \cdot \tan^{-1}\left(\frac{w_{spb}}{u_{spb}}\right) + \Delta\alpha_2 + \eta_{\alpha_{spb}}; \\ \beta_{spb} &= K_{\beta 1} \cdot \sin^{-1}\left(\frac{v_{spb}}{\sqrt{u_{spb}^2 + v_{spb}^2 + w_{spb}^2}}\right) + \Delta\beta_1 + \eta_{\beta_{spb}}; \\ \beta_{npb} &= K_{\beta 2} \cdot \sin^{-1}\left(\frac{v_{npb}}{\sqrt{u_{npb}^2 + v_{npb}^2 + w_{npb}^2}}\right) + \Delta\beta_2 + \eta_{\beta_{npb}} \end{aligned} \tag{8}$$

The density of air ρ can be computed from the actual measurement of static pressure p_s using the universal gas law, ρ = Ps/ (RTs) where R is the gas constant and Ts the static temperature. $k_{\alpha 1}, k_{\alpha 2}, k_{\beta 1}, k_{\beta 2}$, are the scale factors and $\Delta\alpha 1, \Delta\alpha 2, \Delta\beta 1, \Delta\beta 2$ are the biases used to model the measurement errors. These are the sensors calibration parameters obtained by estimation.

The velocity components along the three body-fixed axes at an off CG location are computed from u, v and w as follows:

$$\begin{aligned} u_{offcg} &= u - (r_m - \Delta r)y_{offcg} + (q_m - \Delta q)z_{offcg} \\ v_{offcg} &= v - (p_m - \Delta p)z_{offcg} + (r_m - \Delta r)x_{offcg} \\ w_{offcg} &= w - (q_m - \Delta q)x_{offcg} + (p_m - \Delta p)y_{offcg} \end{aligned} \tag{9}$$

where ($x_{offcg}, y_{offcg}, z_{offcg}$) denote the offset distances from the centre of gravity to the flow angle sensor mounted on the aircraft; (u_{vane},v_{vane},w_{vane}) are the velocity components along the three body-fixed axes corresponding to the flow angle sensor-vane deflection;(u_{spb},v_{spb},w_{spb}) and (u_{npb},v_{npb},w_{npb}) are the velocities components corresponding to side airdata pressure probe and nose boom pressure probe respectively. From the postulated measurement and dynamic models, (6) (7) (8), state, input, measurement and parameter vectors are, respectively.

$$\mathbf{x} = \begin{bmatrix} u & v & w & \phi & \theta & h \end{bmatrix}^T \in \Re^{6};$$
$$\mathbf{u} = \begin{bmatrix} A_x & A_y & A_z & p & q & r \end{bmatrix}^T \in \Re^{6};$$
$$\mathbf{z} = \begin{bmatrix} V_m & \bar{q}_m & \phi_m & \theta_m & h_m & \alpha_{vane} & \alpha_{spb} & \beta_{spb} & \beta_{npb} \end{bmatrix}^T \in \Re^{9};$$
$$\mathbf{\Theta} = \begin{bmatrix} \Delta p, \Delta q, \Delta r, \Delta A_x, \Delta A_y, \Delta A_z, \Delta \bar{q}, K_{\alpha 1}, \\ \Delta\alpha_1, K_{\alpha 2}, \Delta\alpha_2, K_{\beta 1}, \Delta\beta_1, K_{\beta 2}, \Delta\beta_2 \end{bmatrix} \in \Re^{15}; \tag{10}$$

Finally, the EKF extended state vector is defined as

$$\mathbf{x} = \begin{bmatrix} u, v, w, \phi, \theta, h, \Delta p, \Delta q, \Delta r, \Delta A_x, \Delta A_y, \Delta A_z, \Delta \bar{q}, K_{\alpha 1}, \\ \Delta\alpha_1, K_{\alpha 2}, \Delta\alpha_2, K_{\beta 1}, \Delta\beta_1, K_{\beta 2}, \Delta\beta_2 \end{bmatrix} \in \Re^{21}; \tag{11}$$

2.3. Turbulence Model

In case of turbulence in flight, estimated flow angles using above-mentioned state and measurement equations show major variation from simulated flight values. It is mainly due to the model deficiency in the estimation framework. Dynamical representation of atmospheric turbulence is obtained by including Dryden model in the system equations used for estimation. The features that distinguish one turbulence structure from the other are the turbulence intensity σ and integral scale of turbulence L.

In the present investigation L = 1750 ft and σ =10 ft/sec are considered to generate moderate turbulence condition. To account for turbulence in forward velocity, lateral velocity and vertical velocity, the dynamic model considered and appended to the state model in Eq (10) has the following form [20]:

$$\dot{y}_u = \frac{-y_u + x_u k_u \sqrt{\frac{\pi}{\Delta t}}}{t_u};$$
$$\dot{y}_{v_2} = y_{v_1};$$
$$\dot{y}_{v_1} = -\frac{y_{v_2}}{t_v^{\,2}} - \frac{2y_{v_1}}{t_v} + x_v \sqrt{\frac{\pi}{\Delta t}};$$
$$\dot{y}_{w_2} = y_{w_1};$$
$$\dot{y}_{w_1} = -\frac{y_{w_2}}{t_w^{\,2}} - \frac{2y_{w_1}}{t_w} + x_w \sqrt{\frac{\pi}{\Delta t}} \tag{12}$$

where x_u, x_v, x_w random numbers are generated to simulate the random nature of turbulence; $\mathrm{t_u}, \mathrm{t_v}, \mathrm{t_w}, k_\mathrm{u}, k_\mathrm{v}$ and k_w are the time constants that are defined as follows:

$$t_u = \frac{L_u}{V_t}, t_v = \frac{L_v}{V_t}, t_w = \frac{L_w}{V_t}, \text{ where}$$
$$V_t = \sqrt{u^2 + v^2 + w^2};$$
$$\sigma_u = \sigma_v = \sigma_w = \sigma;$$
$$L_u = L_v = L_w = L;$$
$$k_u = \sqrt{\frac{\left(2\sigma_u{}^2 t_u\right)}{\pi}}; k_v = \sqrt{\frac{\left(2\sigma_v{}^2 t_v\right)}{\pi}}; k_w = \sqrt{\frac{\left(2\sigma_w{}^2 t_w\right)}{\pi}}$$

The turbulence in velocity components in flight path axes can now be obtained using the relations [20]:

$$u_{fturb} = y_u;$$

$$v_{fturb} = \frac{k_v}{t_v}\left[\frac{y_{v2}}{t_v} + \sqrt{3}\cdot y_{v1}\right];$$

$$w_{fturb} = \frac{k_w}{t_w}\left[\frac{y_{w2}}{t_w} + \sqrt{3}\cdot y_{w1}\right];$$

Turbulence generated in flight path axes transformed to body axes are given by

$$\begin{bmatrix} u_{bturb} \\ v_{bturb} \\ w_{bturb} \end{bmatrix} = \begin{bmatrix} \cos(\alpha)\cos(\beta) & -\cos(\alpha)\sin(\beta) & -\sin(\alpha) \\ \sin(\beta) & \cos(\beta) & 0 \\ \sin(\alpha)\cos(\beta) & -\sin(\alpha)\sin(\beta) & \cos(\alpha) \end{bmatrix} \cdot \begin{bmatrix} u_{fturb} \\ v_{fturb} \\ w_{fturb} \end{bmatrix}$$

$$\text{where } \beta = \sin^{-1}\left(\frac{v}{V_t}\right) \text{ and } \alpha = \tan^{-1}\left(\frac{w}{u}\right) \tag{13}$$

In the influence of turbulence, the equations relating the states in **x** to the measurement **z** in (10) are modified through replacing u, v and w by, $u - u_{bturb}$, $v - v_{bturb}$ and $w - w_{bturb}$ in (8) respectively.

3. RESULTS

In this section the proposed multi sensor data fusion method is validated via a FPR application using both simulated data with wind/turbulence effects, generated through nonlinear simulation software and flight test data obtained from a high performance fighter aircraft prototype flight test.

In the context of FPR, it is once again pointed out that Q matrix represents input noise and it is not to be confused with atmospheric disturbance. It implies noise in the measurement of the linear accelerations and angular rates, which are in this case the input variables. If the EKF based approach is to be applied to flight data gathered in turbulent atmospheric condition, it requires not only extended Kalman filter, but also simultaneous modeling of atmospheric turbulence. The measurement and input noise covariance matrices (R, Q) are design parameters for the Kalman filter, which were prespecified based on reasonable information obtained from the laboratory calibration of the various measurement sensors. Alternatively, these noise characteristics can also calculated from existing time histories through data filtering. Thus, these noise statistics are generally prespecified, which may not be quite accurate, and therefore may affect the estimates. In order to get the optimal estimate of the states, these noise covariance matrices Q and R were adjusted based on residuals and theoretical innovation bounds analysis.

3.1. Simulated Data Results

Simulated data for pitch stick and rudder doublet inputs were generated at flight condition of Mach 0.3, altitude 1800 meters, with 15-m/sec steady winds at various heading angles (0°, 90°, 180° and 270°) and also for moderate turbulence. Simulated data were corrupted by a time varying input and measurement noise with typical signal to noise levels found in real applications (see Table1). The simulated data were generated at a sampling rate of 0.025sec.

For the sake of defining measurements in simulation AoA and AoSS are computed using the following equations. These measurements are influenced by wind/ turbulence also.

$$\alpha_{m1} = \sin^{-1}\left(\frac{\sin\theta_m}{\sqrt{\sin^2\theta_m + \cos^2\theta_m\cos^2\phi_m}}\right) -$$

$$\sin^{-1}\left(\frac{\frac{\dot{h}_m}{V_m} + \sin\beta_m\sin\phi_m\cos\theta_m}{\left(\sqrt{\sin^2\theta_m + \cos^2\theta_m\cos^2\phi_m}\right)\cos\beta_m}\right)$$

where, $\dot{h}_m = (u-ug)\sin\theta - (v-vg)\sin\phi\cos\theta - (w-wg)\cos\phi\cos\theta$;

$$V_m = \sqrt{(u-ug)^2 + (v-vg)^2 + (w-wg)^2}$$

$$\alpha_{m2} = \frac{\frac{m \cdot A_z}{\bar{q} \cdot S} - C_{z_0}}{C_{z_\alpha}} \quad ; \tag{14}$$

m is the mass of the aircraft and *ug, vg* and *wg* are gust/turbulence velocity components.

$$\beta_m = -\left(A_y - \beta - gain\right) \tag{15}$$

where $\left(A_y - \beta - gai\right.$ is A_y to β gain and is taken from the look up table given as a function of dynamic pressure ($\bar{q}$).

Table 1. Measurement Noise levels used in simulated data

Sensor	Standard deviation, σ	unit
Accelerometers	0.01	m/s^2
Rate gyros	0.0001	rad/s
AoA Measurement-1	0.0003	rad
AoA Measurement-2	0.0002	rad
AoSS Measurement	0.0008	rad
Vertical position	0.012	meter
Dynamic pressure	10	Pa
Euler Angles	0.0002	rad
True airspeed	0.01	m/s

The reconstructed AoA and AoSS slide from estimated states $\hat{u}, \hat{v}, \hat{w}$ are obtained by applying Kalman Filter Technique to each of the data sets with 15 m/sec wind at various heading angles. Here, we have introduced initial state x_0= (99.67587, –0.0196, 25.009, 0.0001, 0.24585, 1800) and state propagation error covariance matrix P_0= diag (100.429, 15, 120.58, 20, 2.0028, 2500). These estimated responses of α and β compare well with the simulated flight data as shown in figures 2 and 3. The

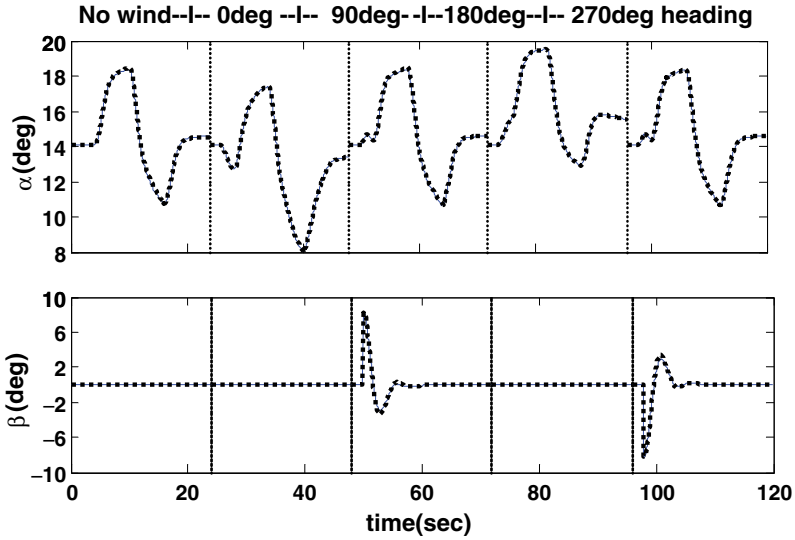

Figure 2. Comparison of Estimated and Flight Simulated Responses: —— Flight simulated and ·····, estimated. [Pitch Stick Doublet with 15 m/s wind at various heading angles]

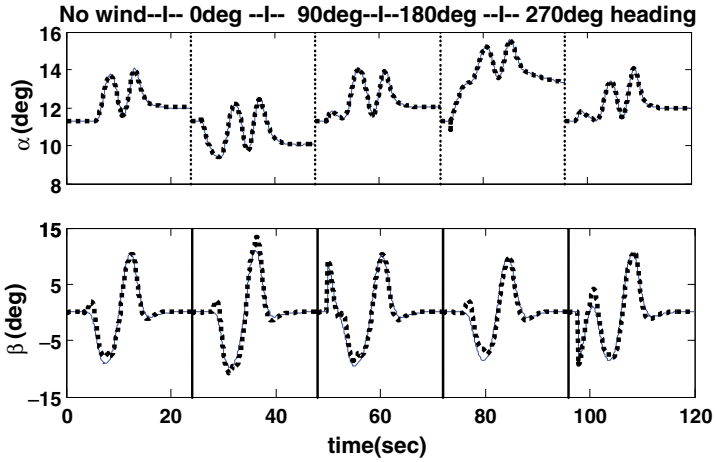

Figure 3. Comparison of Estimated and Flight Simulated Responses: —— Flight simulated and ·····, estimated. [Rudder Doublet with 15 m/s wind at various heading angles]

Calibration parameters of AoA are noted in average as $K_\alpha = 0.9611$, $\Delta\alpha = 0.197$deg for pitch stick doublet and $K_\alpha = 1.1896$, $\Delta\alpha = -2.223$deg for rudder doublet.

In case of moderate level of turbulence, velocity components of turbulence are simulated as shown in Fig 4. Once the filter is tuned, its performance is checked by verifying innovation sequence for zero mean and whiteness [21]. As per these conditions, the 95% of the residual should lie within the bounds, $\pm 2R_{e_{(k)}}^{1/2}$

$$\text{where } Re_{(k)} = C(k)\tilde{P}(k)C_{(k)}^{T} + R$$

and the autocorrelation of the residual should lie within the $\pm 1.96/N^{1/2}$ where N is the number of samples. Along with this, the estimated filter model output with the output measurements are compared to ensure the performance of the filter. Typical results of the autocorrelation and the residual plots for simulated data in turbulence are shown in figures 5 and 6 respectively.

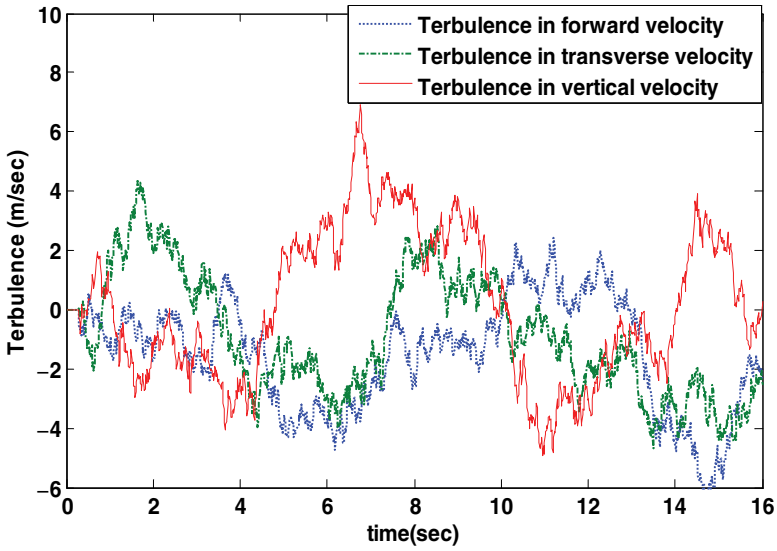

Figure 4. Moderate Turbulence

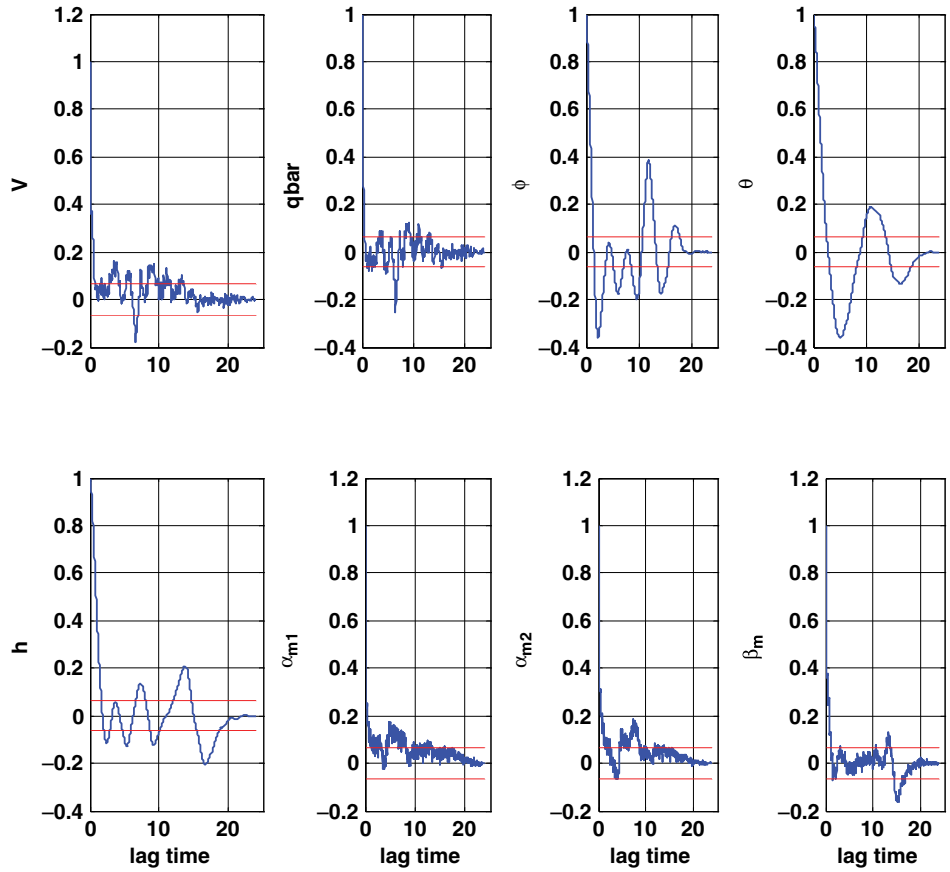

Figure 5. Autocorrelation of residual with bounds [Whiteness test]

The investigations are made with and without augmented turbulence model in estimation framework. It is found that estimation of α and β for both cases of pitch stick and rudder doublet, with augmented states yields better result as shown in figure 7. The Calibration parameters of AoA are $K_\alpha = 1.1571$, $\Delta\alpha = -1.782$deg for pitch stick doublet and $K_\alpha = 0.9953$, $\Delta\alpha = -0.06876$deg for rudder doublet. The minor differences in the response match of AoSS for the rudder doublet are attributed primarily to the use of single computed AoSS as a measurement. It can be further improved by fusing the additional measurement data of AoSS in the estimation. Nevertheless, the agreement between the estimated and simulated flight responses is very encouraging to apply on flight test data.

3.2. Flight Test Data Results

To evaluate the proposed data fusion method in a real condition, high performance fighter aircraft prototype was used to generate the data necessary for the analysis. Dynamic maneuvers (doublets, 3211, pull up and AoA sweep) for the variation of mach from 0.39 to 0.95 and altitude from 2000 to 14000 meters, AoA excursions up to 21deg and AoSS excursions up to ±5deg were selected. The sampling period adopted was 0.025 second. The analysis of flight maneuvers for various Mach numbers were carried out separately mainly because, from a priori knowledge, the sensitivity factor is expected to vary with speed. Figure 8 shows variation of sensitivity factors and offset errors estimated separately from maneuvers at different Mach numbers. It is observed that correction factors show a clean reduction for higher values of Mach numbers. Absolute values of the filter estimation errors with time are shown in figure 9 for the entire flight measured data analyzed.

It is required to validate the sensor data fusion approach by comparing with standard technique of FPR using the output error method (OEM).The output error method is successively applied to estimate the sensitivity factor and bias of calibration parameters and use to correct the measurements AoA and AoSS. The corrected angle of attack and angle of sideslip values are to be used as references; the filter results are compared against calibrated data based on reference method OEM [16]. The application of

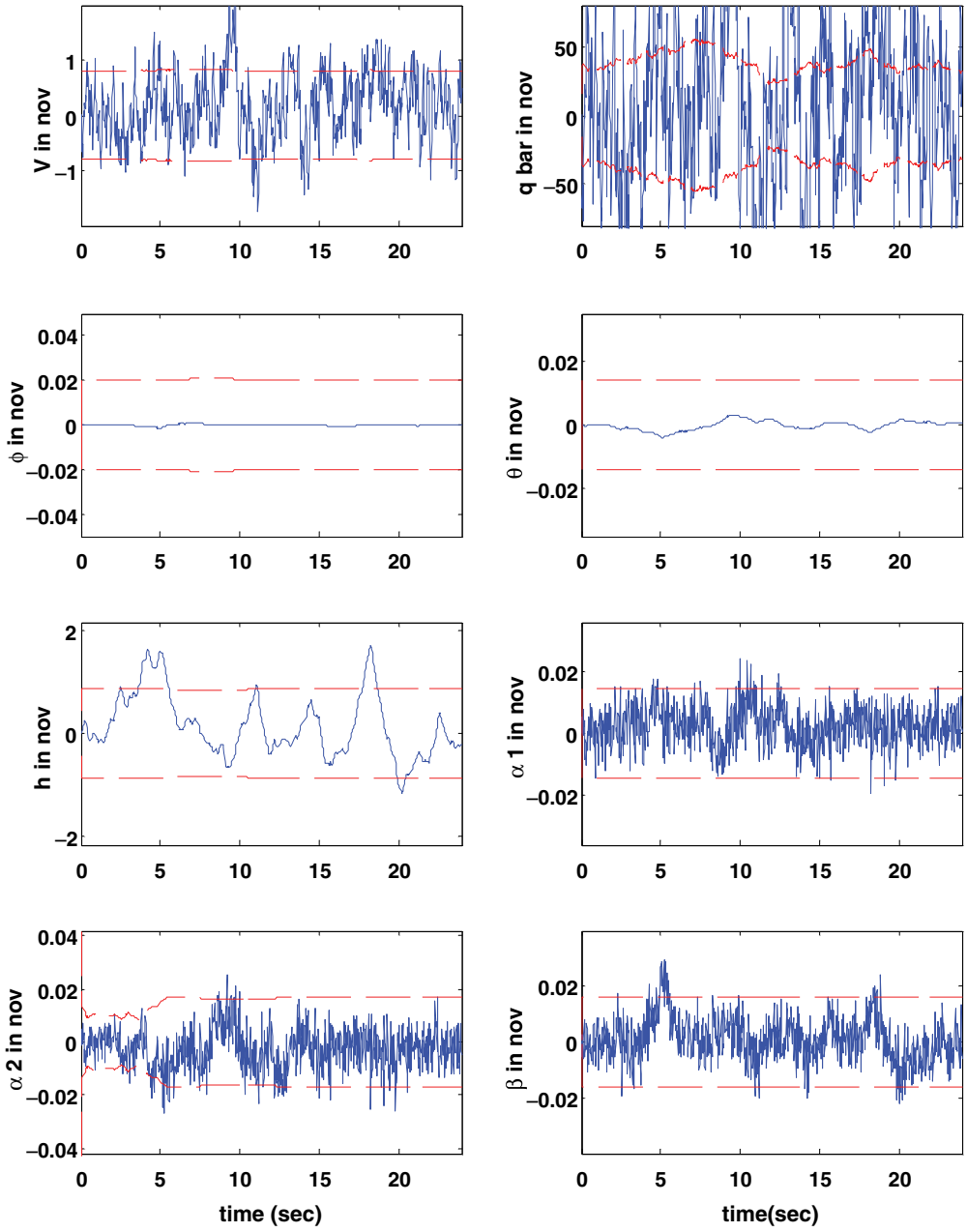

Figure 6. Residual with two sigma bounds

OEM for FPR is omitted here for brevity. The difference between AoA, AoSS estimated using sensor data fusion based approach and those obtained using OEM based method is shown in figure 10.

The variation of estimation errors of alpha and beta are respectively, almost around aerospace industry requirement values ±0.5deg and ±0.25deg except at some certain points. The larger error in AoA and AoSS at these points is due to mismatch in the initial values of the maneuvers. Of course this initial value problem does not arise for the online application of EKF based sensor fusion algorithm.

The discrepancy of flow angle sensors was noted as high for the AoA sweep maneuver (i.e., see Fig. 7, from 75sec to 125sec) compared to other dynamic maneuvers. Hence the initial mismatches of estimated flow angles for that maneuver can observe from the figure 10 at 75 sec wherein estimated AoA error is more than ±0.5deg.

During this significant variation of sensors measurement noise property, degree of estimation accuracy also depends upon the number of sensors employed for measurements in sensor fusion. In the presence of wind or atmospheric disturbances, the estimation accuracy can be further improved by

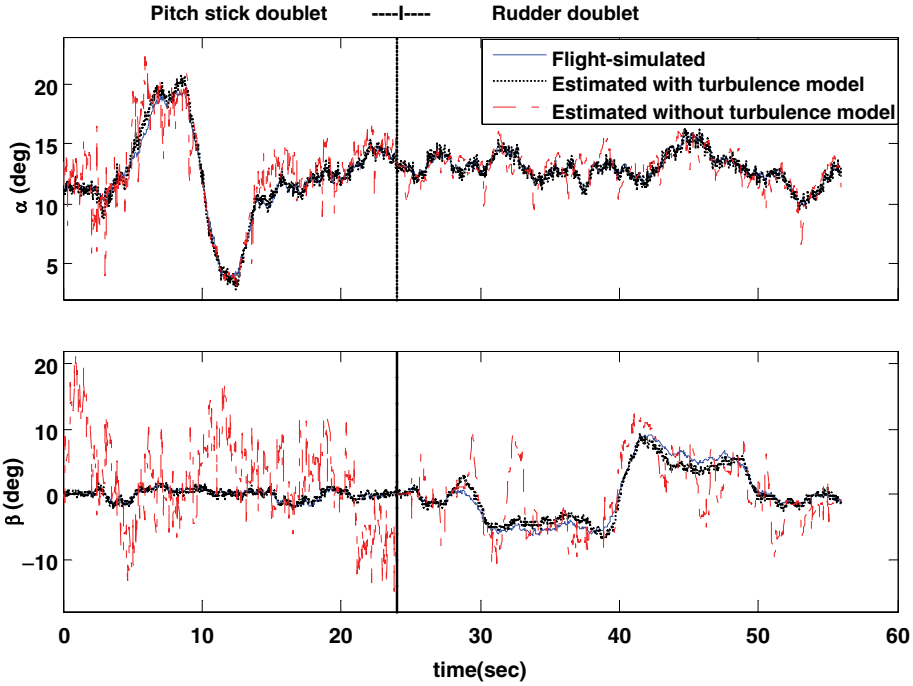

Figure 7. Comparison of Estimated and Flight simulated Flow angles [With and without augmented turbulence model]

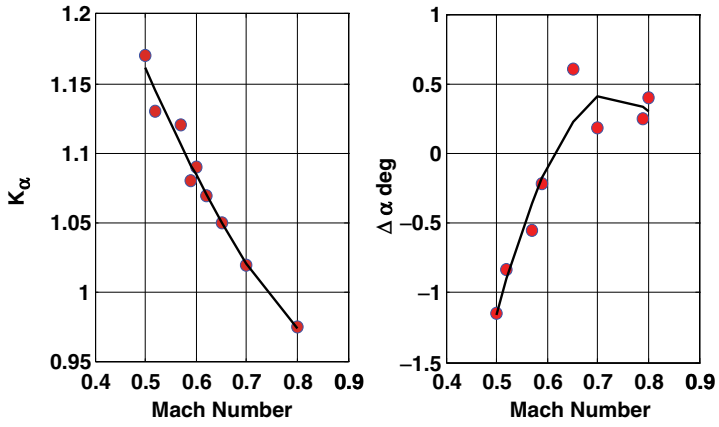

Figure 8. Filter Estimated Calibration Parameters of AoA

introducing more number of accurate sensors for EKF based data fusion and it is of great value in online practice as EKF having the property of real time estimation.

4. CONCLUSIONS

This paper describes the application of Extended Kalman filtering technique in sensor fusion algorithm to calibrate the angle of attack and angle of sideslip in real time from both simulated and real flight test data of a high performance aircraft. Simulations in software were carried out with 15 m/sec wind effects at 1800 meters altitude and 0.3 Mach to obtain sufficient variations in α, β of the aircraft. The investigations are initially made from simulated data with wind and turbulence effects using Simulation Software and showed that estimated both α and β are accurate. In the case of turbulence, it is found that estimation of AoA and AoSS with augmented states yields better results. The same procedure is extended to real time flight test data of a high performance aircraft. It is observed that sensor fusion algorithm provides estimation accuracy almost around ±0.5deg and ±0.25deg, respectively for AoA and AoSS and shows sensor fusion approach proposed in this paper is of great value in online practice.

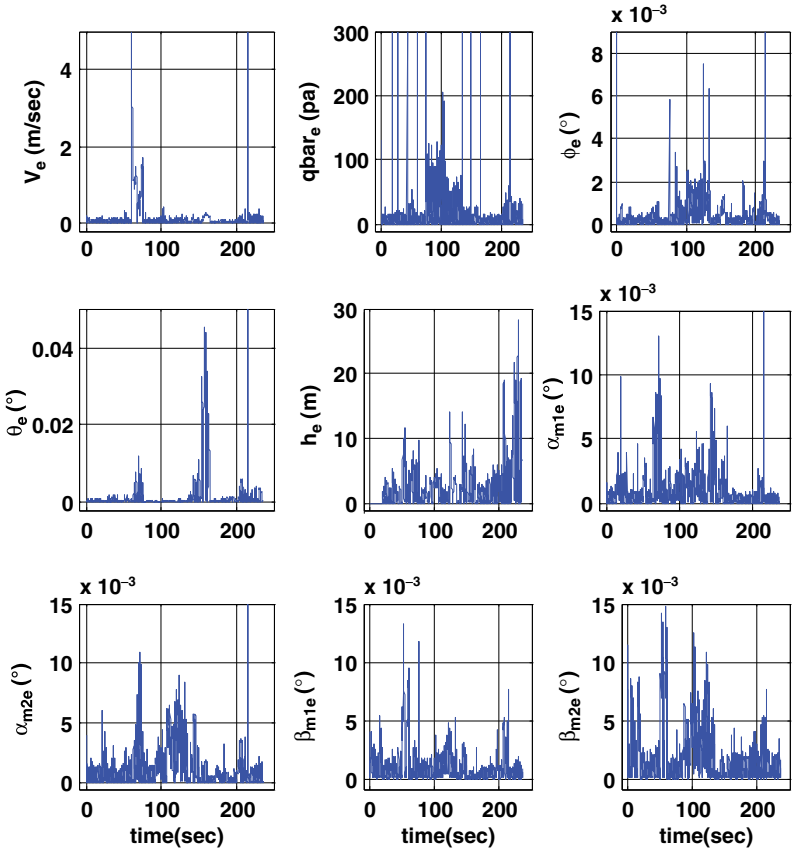

Figure 9. EKF Estimation Absolute Errors

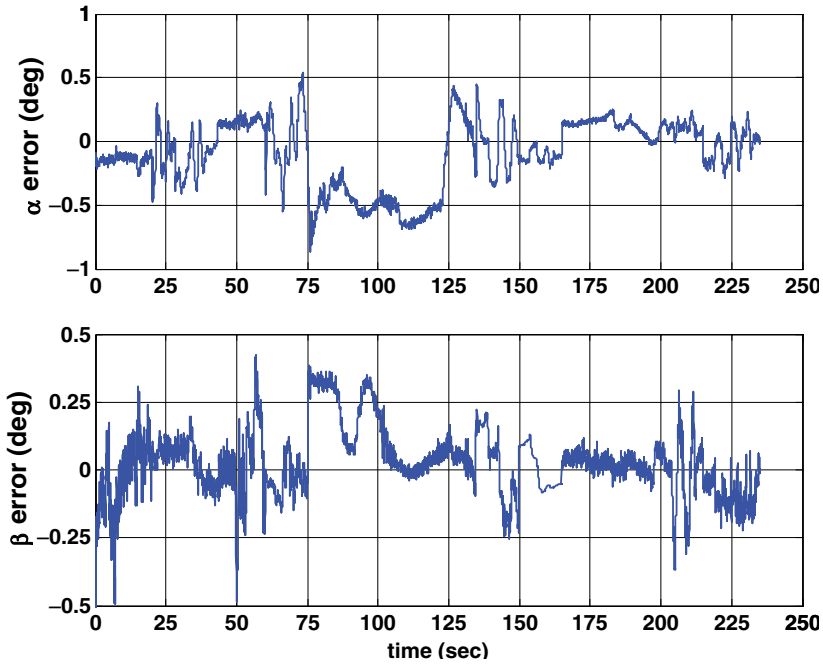

Figure 10. Filter Estimated Errors of AoA and AoSS

5. ACKNOWLEDGEMENTS

The authors are grateful to Dr. Amitabh Saraf, Scientist-F, ADA, Bangalore and Dr. Jatinder Singh, Scientist-F, NAL, Bangalore for their encouragement and technical discussion during the course of work. The authors also gratefully acknowledge Mr. Shyam Chetty, Head, Flight Mechanics and Control Division of National Aerospace Laboratories, Bangalore for his moral support.

6. REFERENCES

1. Menzies, M. A., "Integrated Air Data Sensors", The Aeronautical Journal, Vol. 105, Apr. 2001, pp.223-229.
2. Parameswaran V., Jategaonkar R.V, M. Press., "Five-Hole Flow Angle Probe Calibration from Dynamic and Tower Flyby Maneuvers", Journal of aircraft,, Vol. 42, No. 1, January–February 2005.
3. Edward A., Haering, Jr., "Air data Measurement and Calibration", NASA-TM 104316, December 1995.
4. Marco Lando, Manuela and Piero., " Neuro-Fuzzy Techniques for the Air-Data Sensor Calibration", Journal of Aircraft, Vol. 44, No.3, May-June 2007.
5. Chu QP, Mulder JA, Van Woerkom PThLM., "Modified recursive maximum likelihood adaptive filter for nonlinear aircraft flight-path reconstruction". AIAA J. Guidance Control Dyn 1996; 19(6):1285-95.
6. Kevin A. Wise, "Flight Testing of the X-45 A J-UCAS Computational Alpha-Beta System", AIAA 2006-6215, 2006.
7. David L. Hall, "Mathematical Techniques in Multi sensor Data fusion," Artech House, 2004.
8. Bar-Shalom, Y., and Fortmann, T.E, "Tracking and Data Association", New York: Academic Press, 1998.
9. Saha,R.K, "Track-to-track fusion with dissimilar sensors", *IEEE Transactions on Aerospace and Electronic Systems,* 34,3(1996), 1021-1029.
10. Hui, K.,Srinivasan,R., and Baillie, S., "Simultaneous Calibration of Aircraft Position Error and Airflow Angles Using Differential GPS", Canadian Aeronautics and Space Journal, Vol. 42, No.4, Dec. 1996, pp. 185-193.
11. Roecker J. A., and McGillem, C. D., " Comparison of two sensor tracking methods based on sate-vector fusion and measurement fusion", *IEEE Transactions on Aerospace and Electronic Systems,* 24,4 (1988), 447-449.
12. Qiang Gan and Chris J.Harris, "Comparison of two measurement fusion methods for Kalman-filter-based multisensor data fusion", *IEEE Transactions on Aerospace and Electronic Systems,* Vol. 37 No.1 January 2001.
13. Celso Braga de M, Elder Moreina H and Luiz Carlos SG, "Adaptive Stochastic Filtering for Online Aircraft Flight Path Reconstruction", Journal of aircraft, Vol. 44, No.5, Sept-October 2007.
14. Klein, V., and Schiess, J. R., "Compatibility Check of Measured Aircraft Responses Using Kinematic Equations and Extended Kalman Filter," NASA TN D-8514, Aug. 1977.
15. Keskar, D. A., and Klein, V., "Determination of Instrumentation Errors from Measured Data Using Maximum Likelihood Method," AIAA Paper80-1602, 1980.
16. Maine, R. E., and Iliff, K. W., "Identification of Dynamic Systems Applications to Aircraft". Part 1: The Output Error Approach," AG-300, AGARD, Vol. 3, Pt. 1, Dec. 1986.
17. Hamel, P. G., Jategaonkar, R.V., "Evolution of Flight Vehicle System Identification," Journal of Aircraft, Vol. 33, No. 1, 1996, pp. 9–28.
18. Maybeck,P.S., "Stochastic Models, Estimation, and Control," Vol. 1. Academic Press, New York, 1979.
19. Jategaonkar, R.V., "Flight Vehicle system Identification: A time domain Methodology", Vol. 216, AIAA Progress in Astronautics and Aeronautics Series, AIAA, Reston, VA, Aug. 2006.
20. Marvin, Joseph G., "Dryden Lectureship in Research- A perspective on CFD validation", Aerospace Sciences Meeting, 31st, Reno, NV, Jan 11-14, AIAA-1993-2.
21. James V. Candy., "Signal Processing: A Modern Approach", International Edition 1988.